Acta Biomaterialia 80 (2018) 288–295

Contents lists available at ScienceDirect

Acta Biomaterialia

journal homepage: www.elsevier.com/locate/actabiomat

Full length article

Hyaluronic acid shell and disulfide-crosslinked core micelles for in vivo targeted delivery of bortezomib for the treatment of multiple myeloma

Zhaoxin Gu [a], Xiuxiu Wang [a], Ru Cheng [a,*], Liang Cheng [a,b], Zhiyuan Zhong [a,*]

[a] Biomedical Polymers Laboratory, and Jiangsu Key Laboratory of Advanced Functional Polymer Design and Application, College of Chemistry, Chemical Engineering and Materials Science, Soochow University, Suzhou 215123, PR China
[b] Department of Pharmaceutics, College of Pharmaceutical Sciences, Soochow University, Suzhou 215123, PR China

ARTICLE INFO

Article history:
Received 4 June 2018
Received in revised form 3 September 2018
Accepted 15 September 2018
Available online 19 September 2018

Keywords:
Multiple myeloma
Proteasome inhibitor
Targeted delivery
CD44
Reduction-sensitive
Micelles

ABSTRACT

Bortezomib (BTZ) provides one of the best treatments for multiple myeloma (MM). The efficacy of BTZ is, nevertheless, restricted by its fast clearance, low selectivity, and dose limiting toxicities. Here, we report on targeted BTZ therapy of MM in vivo by hyaluronic acid-shelled and core-disulfide-crosslinked biodegradable micelles (HA-CCMs) encapsulating lipophilized BTZ, bortezomib-pinanediol (BP). HA-CCMs loaded with 7.3 BTZ equiv. wt% exhibited a small size of 78 nm, good stability in 10% FBS, and glutathione-triggered drug release. MTT assays in CD44 positive LP-1 multiple myeloma cells revealed that BP encapsulated in HA-CCMs caused enhanced antiproliferative effect compared with free BP. Flow cytometry, confocal microscopy and MTT assays indicated BP-loaded HA-CCMs (HA-CCMs-BP) could actively target to LP-1 cells and induce high antitumor effect. Proteasome activity assays in vitro showed HA-CCMs-BP had a similar proteasome activity inhibition as compared to free BTZ at 18 h. The fluorescence imaging using Cy5-labeled HA-CCMs showed that HA-CCMs had a long elimination half-life and enhanced tumor accumulation via HA-mediated uptake mechanism. The therapeutic studies in LP-1 MM-bearing mice revealed better treatment efficacy of HA-CCMs-BP compared with free BTZ, in which HA-CCMs-BP at 3 mg BTZ equiv./kg brought about significant tumor growth inhibition and survival benefits. Loading of lipophilized BTZ into HA-shelled multifunctional micelles has emerged as an exciting approach for bortezomib therapy of MM.

Statement of Significance

Multiple myeloma (MM) is the second most common hematological malignancy. Bortezomib (BTZ), a potent proteasome inhibitor, provides one of the best treatments for MM. The clinical efficacy of BTZ is, however, limited by its quick clearance, poor selectivity, and significant side effects including myelosuppression and peripheral neuropathy. Here, we report on targeted BTZ therapy of MM in vivo by hyaluronic acid-shelled and core-disulfide-crosslinked biodegradable micelles (HA-CCMs) encapsulating lipophilized BTZ, bortezomib-pinanediol (BP). Our results showed that BP-loaded HA-CCMs exhibit markedly enhanced toleration, broadened therapeutic window, and significantly more effective growth suppression of CD44-overexpressed multiple myeloma in nude mice than free bortezomib. Lipophilized BTZ-loaded HA-CCMs has opened a new avenue for targeted bortezomib therapy of multiple myeloma.

1. Introduction

Multiple myeloma (MM) is the second most common hematological malignancy [1–3]. Bortezomib (BTZ), a potent proteasome inhibitor, provides one of the best treatments for MM [4,5]. BTZ takes effect by binding to the threonine residues in the proteasome and thereby preventing degradation of pro-apoptotic proteins, leading to programmed death of cancerous cells [6–8]. The clinical efficacy of BTZ is, however, limited by its quick clearance, bad selectivity, and quite a few side effects including myelosuppression and peripheral neuropathy [9–11]. Notably, peripheral neuropathy occurs in approximately 30% of patients while myelosuppression may pose dose-limiting effect.

* Corresponding authors.
E-mail addresses: rcheng@suda.edu.cn (R. Cheng), zyzhong@suda.edu.cn (Z. Zhong).

https://doi.org/10.1016/j.actbio.2018.09.022
1742-7061/

To increase its therapeutic efficacy and reduce systemic toxicity, BTZ has been formulated as polymer-drug conjugates or with different carrier systems including micelles, liposomes, and nanoparticles [12–21]. For example, taking advantage of its boronic acid functional group, BTZ prodrugs were obtained by linking BTZ to polymers via pH-sensitive boronate ester bonds [22,23]. These BTZ prodrugs showed improved pharmacokinetics and pH-dependent BTZ release though they exposed a low aqueous stability and fast hydrolytic degradation. Liposomal BTZ demonstrated proteasome inhibition against MM cell lines in vitro and reduced systemic toxicity compared to free BTZ in vivo though improvement of anti-tumor efficacy was not significant [21]. Interestingly, Ghobrial et al. reported that alendronate-decorated PEG-PLGA nanoparticulate BTZ with drug loading contents (DLC) of 0.04–0.74 wt% and active bone-targeting showed enhanced survival and decreased tumor burden in mouse model of MM compared to free BTZ [15]. It is noted, however, that nearly all reported nanosystems revealed a deficient loading for BTZ [17–19], likely related to its amphipathic nature, as well as low selectivity to MM. Interestingly, Zuccari et al. sequentially loaded aminolactose and BTZ formed boronate esters into liposomes, leading to enhanced BTZ loading of 3.56 wt% [20]. Wang et al. achieved a good BTZ loading of 7.28 wt% in PEG-*b*-poly(D,L-lactide) (PEG-PLA) nanoparticles by single emulsion method [16]. We recently found that lipophilized bortezomib (BP), could be efficiently loaded into micelles, giving enhanced treatment of breast tumor with reduced adverse effects compared with free BTZ [24].

Here, we report on targeted bortezomib therapy of MM in vivo by BP-loaded, hyaluronic acid-shelled and core-disulfide-crosslinked biodegradable micelles (HA-CCMs-BP) (Scheme 1). HA is capable of actively targeting to the CD44-overexpressed solid tumors such as ovarian, breast, prostate, and lung tumors [25–28]. Notably, CD44 presents not only on hematological cancer cells but also on human hematological cancer stem cells [29–31], rendering CD44 a particularly appealing target for hematological cancer therapy. HA-CCMs were readily obtained by self-assembly from a single copolymer, HA-*b*-poly(trimethylene carbonate-*co*-dithiolane trimethylene carbonate) (HA-P(TMC-*co*-DTC)) [32]. Our results showed that HA-CCMs-BP could actively target to LP-1 MM cells, inducing effective proteasome inhibition and enhanced antiproliferative effect compared with free BTZ. HA-CCMs-BP demonstrated superior treatment of LP-1 tumor-bearing mice to free BTZ. HA-CCMs-BP with high drug loading, great simplicity and multifunctionality provides a better and potentially viable treatment for human multiple myeloma.

2. Experimental

2.1. Preparation and characterization of HA-CCMs-BP

The blank HA-CCMs were conveniently prepared by solvent exchange method. Typically, 100 μL of HA-P(TMC-*co*-DTC) polymer solution in DMSO (10 mg/mL) was added into 900 μL phosphate buffer (PB, 10 mM, pH 7.4) under stirring at r.t.. The micelles self-crosslinked at 37 °C for 12 h, and dialyzed against the same PB for 6 h. The dialysis medium was changed per hour. The preparation of HA-CCMs-BP was similar to that of blank HA-CCMs except the organic phase was a mixture of polymer (10 mg/mL in DMSO) and BP (10 mg/mL in DMSO). To determine the DLC and drug loading efficiency (DLE), HA-CCMs-BP suspensions were freeze-dried,

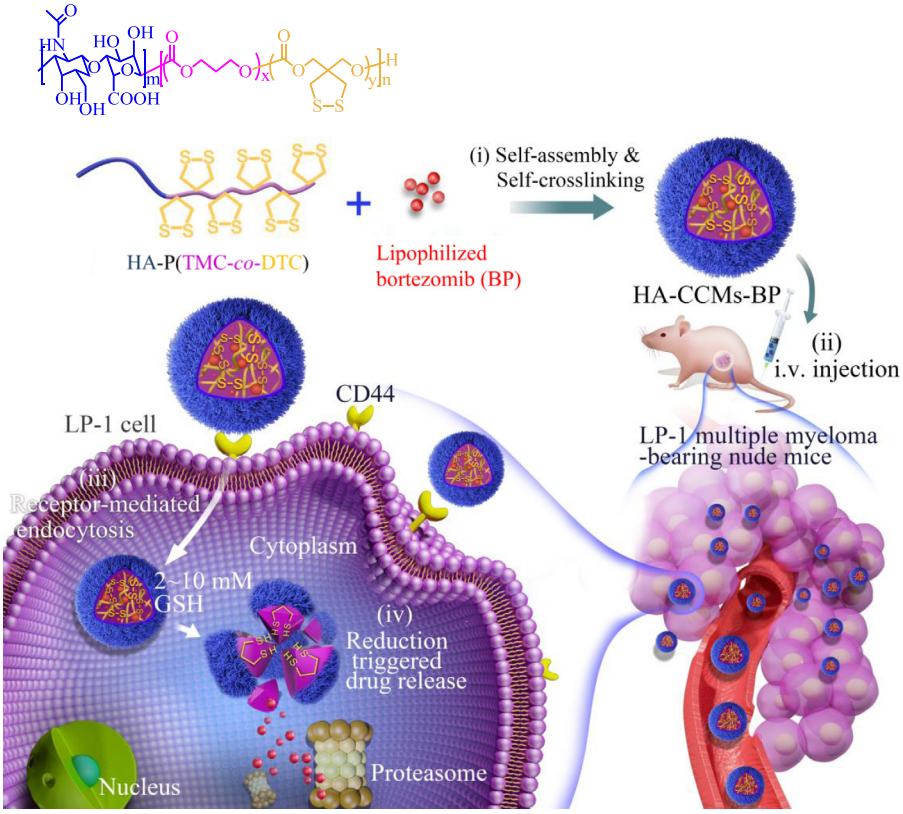

Scheme 1. Schematic design of hyaluronic acid-shelled and core-disulfide-crosslinked biodegradable micelles (HA-CCMs) for targeted delivery of lipophilized bortezomib, bortezomib-pinanediol (BP), to LP-1 multiple myeloma. (i) BP is readily loaded into micelles during self-assembly process and micelles are self-crosslinked during workup, affording robust HA-CCMs-BP; (ii) HA-CCMs-BP following i.v. injection can be long circulating and efficiently accumulate in LP-1 multiple myeloma; (iii) HA-CCMs-BP is taken up by LP-1 cells via a CD44-mediated endocytosis mechanism; and (iv) HA-CCMs-BP is self-de-crosslinked inside the tumor cell, resulting in quick cytoplasmic release of BP and effective inhibition of cell growth.

dissolved in acetonitrile with 10 mM DTT and analyzed using HPLC (acetonitrile/H_2O (70/30, v/v), 1.0 mL/min, UV: 272 nm). DLC and DLE were determined using the following equations:

$$\text{DLC (wt\%)} = (\text{weight of loaded drug/total weight of polymer and loaded drug}) \times 100$$

$$\text{DLE (\%)} = (\text{weight of loaded drug/weight of drug in feed}) \times 100$$

The stability of HA-CCMs-BP in the presence of 10% fetal bovine serum (FBS) was evaluated by monitoring the size change of micelles via DLS. Samples were maintained at 37 °C in a shaking bath at 200 rpm for 12 h. The sizes were monitored at desired time intervals by DLS. HA-CCMs-BP in the absence of 10% FBS was used as a control.

2.2. In vivo imaging and pharmacokinetic studies

Tumors were allowed to grow to an average volume of about 200 ~ 300 mm^3 in diameter before the experiment. HA-CCMs-Cy5 (0.5 μg Cy5 equiv./mouse) was intravenously injected into the tail vein of mice. After the mice were anesthetized with pentobarbital sodium (10 mg/mL in PBS) at a dosage of 62.5 mg/kg, the fluoresce imaging was acquired at different time points (4, 6, 8, 12, and 24 h) using a fluorescence imaging system (IVIS, Lumina II; Caliper, MA; ex. 646 nm and em. 670 nm). The mice in control group were injected with free HA (50 mg/kg, 8 KDa) 0.5 h prior to the administration of HA-CCMs-Cy5. We have cropped out LP-1 tumor sections separately in order to clearly reveal targetability of HA-CCMs-Cy5.

To study the pharmacokinetic of HA-CCMs, HA-CCMs-Cy5 (0.5 μg Cy5 equiv./mouse) was intravenously injected to Balb/C mice. Blood samples were collected by drawing 75 μL blood from the eye socket of mice at different time points (0.08, 0.25, 0.5, 1, 2, 4, 8, 12, and 24 h) and centrifuged at 3000 rpm for 5 mins. Aliquots (20 μL) of plasma were dissolved in100 μL of Triton X-100 (1%) and 400 μL DMSO with 20 mM DTT in the dark overnight. The Cy5 amount in plasma at different time point was determined by fluorescence spectrometer measurement. Its blood circulation follows a two compartment model. The half-lives of two phases ($t_{1/2,\alpha}$ and $t_{1/2,\beta}$) were calculated according to the following formula:

$$y = A_1 \times \exp(-\alpha_1 \cdot t_1) + A_2 \times \exp(-\beta_2 \cdot t_2) + C_0$$
$$t_{1/2,\alpha} = 0.693 \times t_1$$
$$t_{1/2,\beta} = 0.693 \times t_2$$

2.3. In vivo therapeutic efficacy

The in vivo antitumor efficacy of HA-CCMs-BP was performed on LP-1 multiple myeloma tumor-bearing mice. When tumor grew to about 100 mm^3, the mice were randomly divided to five groups: PBS, free BTZ (dosage: 0.5 mg/kg), and HA-CCMs-BP (dosage: 0.5, 1.0, and 3.0 mg BTZ equiv./kg) (n = 6). All the mice were intravenously injected via the tail vein for 2 courses (first course on day 1, 4, 8, 11, and second course on day 19, 22, 26, 29). The tumor size was measured every 2 days, and volume was calculated according to the formula $V = 0.5 \times L \times W^2$. Relative tumor volumes were calculated as V/V_0 (V_0 and V are the tumor volume on day 1 and at any given day, respectively). The mice were weighted every 2 days and their relative body weights were normalized to their initial weights. When the treatment was terminated, one mouse of each group was sacrificed by cervical vertebra dislocation. The major organs and tumors were isolated, fixed with 20% formaldehyde solution for 48 h, embedded in paraffin, and cut into 5-micronmeter thick slices. The tissue slices were mounted on the glass slides, stained by hematoxylin and eosin (H&E) and observed using a digital microscope (Olympus BX41).

2.4. Statistical analysis

Data were expressed as mean ± SD. Differences between groups were assessed by one-way ANOVA with Tukey multiple comparison tests. Survival data were analyzed by the Kaplan-Meier technique with a log-rank test for comparison using Graphpad Prism 7. $^{*}p < 0.05$ was considered significant, and $^{**}p < 0.01$, $^{***}p < 0.001$ were considered highly significant.

3. Results and discussion

3.1. Preparation and characterization of HA-CCMs-BP

HA-CCMs-BP was readily prepared from self-assembly of HA-P(TMC-*co*-DTC) copolymer (M_n = 8.0-(4.5/1.6) kg/mol) with BP in PB (10 mM, pH 7.4) followed by self-crosslinking. Good BP loading, corresponding to 2.8–7.3 BTZ equiv. wt%, was obtained for HA-CCMs-BP at theoretical DLC of 5–20 wt% (Table 1). Both drug loading content and efficacy were significantly higher than previously reported for micellar BTZ (BTZ loading typically <1 wt%) [15,16]. The enhanced drug loading observed for HA-CCMs-BP can be contributed to enhanced hydrophobic interaction between drug and micellar core as well as core crosslinking [24,33,34]. HA-CCMs-BP had small sizes of 76–80 nm and narrow PDI (0.10–0.12) (Table 1). DLS measurement showed little change of micelle size and PDI after 12 h incubation with 10% FBS (Fig. 1A), implying that HA-CCMs-BP has good colloidal stability likely resulting from disulfide crosslinking of micellar core [35–38].

Fig. 1B shows that under physiological conditions about 20% BP was released from HA-CCMs-BP in 24 h, whereas more than 80% BP was released upon adding 10 mM GSH. In comparison, BTZ-encapsulated nanoparticles typically showed a sustained release. For example, ca. 75% drug was released in 7 days under physiological conditions from alendronate coated PLGA nanoparticles, and ca. 30% drug was released in 24 h from PEG-*b*-PLA nanoparticles

Table 1
Characterization of HA-CCMs-BP.

Entry	DLC (BTZ equiv. wt%)		DLE (%)	Size[b] (nm)	PDI[b]
	theory	determined[a]			
1	5	2.8	55.9	76	0.10
2	10	5.1	50.8	80	0.12
3	20	7.3	40.1	78	0.10

[a] Determined by HPLC.
[b] Determined by DLS.

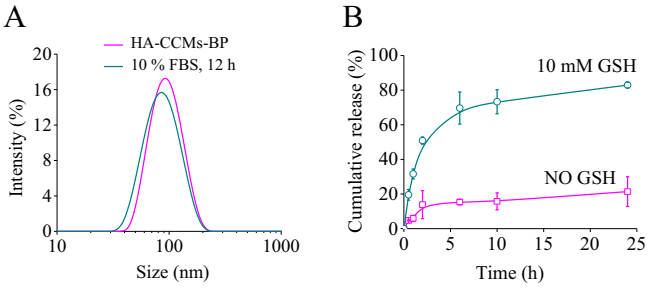

Fig. 1. (A) Colloidal stability of HA-CCMs-BP against 10% FBS. Initial HA-CCMs-BP concentration was 1 mg/mL. (B) *In vitro* release of BP from HA-CCMs-BP with or without 10 mM GSH. Data are presented as mean ± SD (n = 3).

[16,17]. These results indicate that HA-CCMs-BP possesses good stability and fast reduction-triggered drug release behavior.

3.2. Cellular uptake, in vitro antitumor effect, and proteasome activity inhibition of HA-CCMs-BP

To investigate cellular internalization, HA-CCMs were labeled with cyanine 5 (Cy5) (HA-CCMs-Cy5). Confocal microscopy displayed that LP-1 cells following 4 h incubation with HA-CCMs-Cy5 had strong Cy5 fluorescence in the cytosol and perinuclear regions, which was obviously higher than cells pretreated with 5 mg/mL HA (Fig. 2A), corroborating CD44-mediated endocytosis of HA-CCMs. To confirm Cy5 fluorescence indeed from the cytosol, we further stained membrane with rhodamine B-labeled phalloidin and performed z-stack imaging. Fig. S1 shows clearly that Cy5 fluorescence is neither coming from near the top of the cell nor the micelles on the cell membrane. The quantitative flow cytometry analyses showed that after 4 h incubation HA-CCMs-Cy5 group showed nearly 2 times stronger fluorescence in LP-1 cells than HA pretreated control group (Fig. 2B), supporting that HA-CCMs-Cy5 can actively target to CD44-overexpressed LP-1 cells. HA, a biocompatible and biodegradable natural polysaccha-

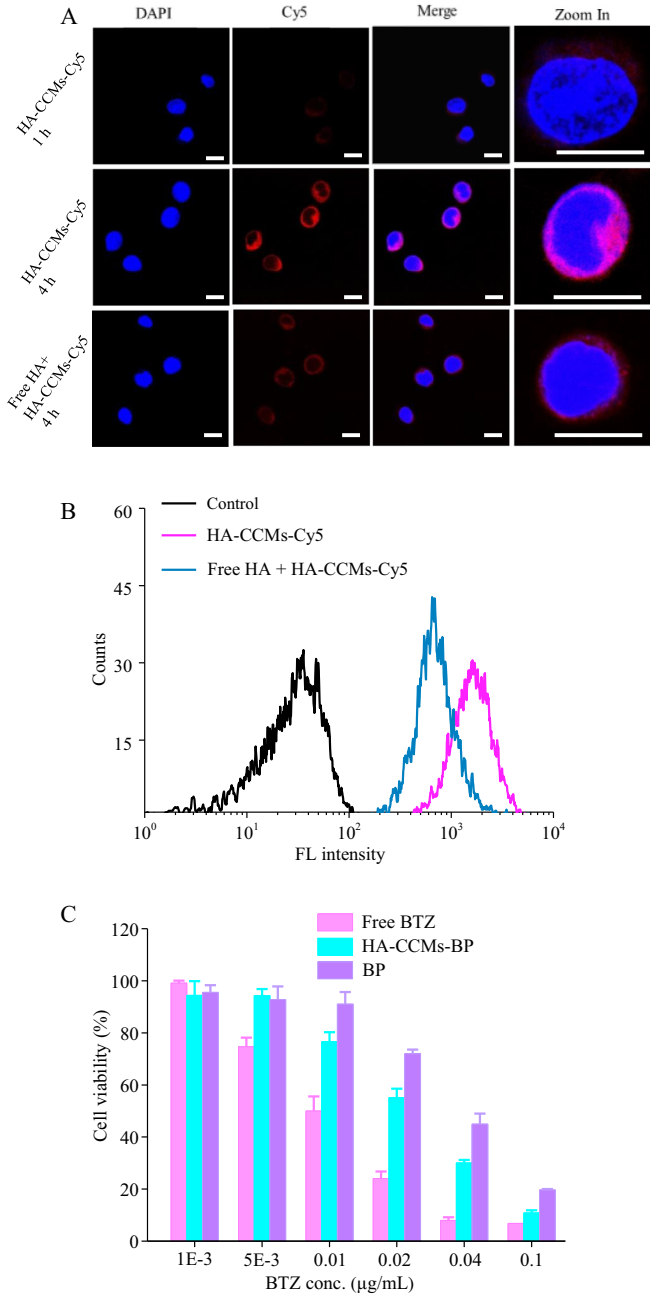

Fig. 2. (A) CLSM images of LP-1 cells after 1 and 4 h incubation with HA-CCMs-Cy5. Scale bar: 10 μm. (B) Flow cytometry of LP-1 cells after 4 h incubation with HA-CCMs-Cy5. The inhibitive experiments were conducted by pretreatment of cells with 5 mg/mL of free HA for 4 h. (C) MTT assays of free BTZ, HA-CCMs-BP and BP in LP-1 cancer cells. The cells were incubated with different formulations for 4 h and cultured in fresh medium for another 44 h (n = 4).

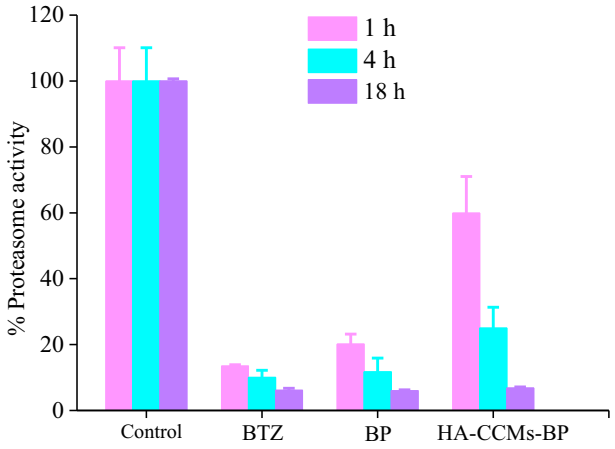

Fig. 3. *In vitro* proteasome activity inhibition assays in LP-1 cells. Cells were incubated with PBS, free BTZ, BP or HA-CCMs-BP for 1, 4, or 18 h (dosage: 20 ng BTZ equiv./mL).

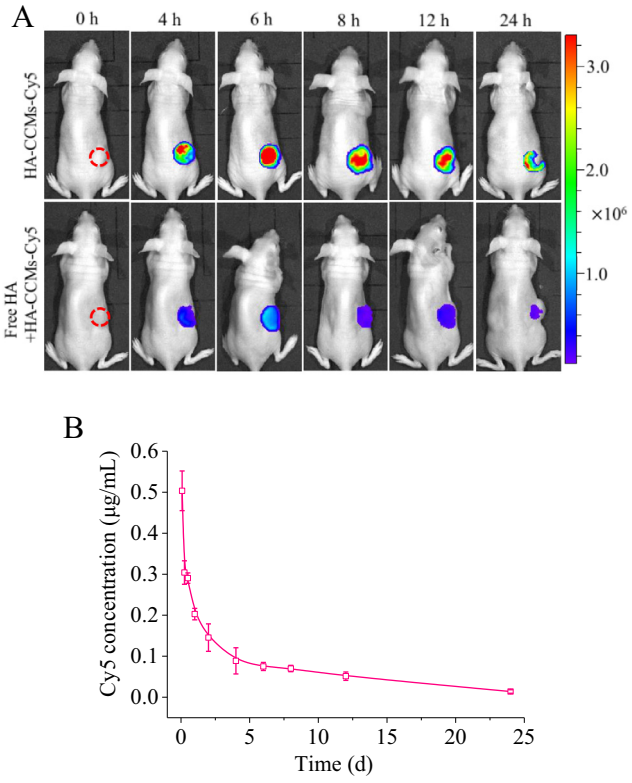

Fig. 4. (A) *In vivo* fluorescence images of LP-1 tumors cropped out from nude mice at different time points after i.v. injection of HA-CCMs-Cy5. Free HA (50 mg/kg) pretreated mice were used as a control. (B) *In vivo* pharmacokinetics of HA-CCMs-Cy5 in Balb/C mice.

ride, has an inherent affinity to CD44 overexpressed in many tumor cells [39–42], including hematological cancer cells [43].

To evaluate the cytotoxicity of HA-CCMs-BP, MTT assays were conducted in CD44 overexpressing LP-1 cells. The results showed that BTZ, BP and HA-CCMs-BP all displayed a concentration-dependent toxicity (Fig. 2C). Notably, BP was less toxic to LP-1 cells than BTZ, as also observed for MDA-MB-231 breast tumor cells [24]. HA-CCMs-BP showed, however, much better antitumor effect than free BP, with a half-maximal inhibitory concentration (IC_{50}) of 0.023 μg/mL, supporting that HA-CCMs-BP can be efficiently internalized by LP-1 cells and quickly release BP into their cytosols. MTT assays showed that blank HA-CCMs induced little reduction of cell viability (Fig. S2), supporting their low cytotoxicity. The active targeting property of HA-CCMs-BP combined with comparably lower toxicity of free BP makes HA-CCMs-BP highly advantageous over BTZ for MM therapy.

We further performed proteasome inhibition assays in LP-1 cells following 1, 4 or 18 h incubation with free BTZ, BP or HA-CCMs-BP at 20 ng BTZ equiv./mL. The results indicated a time-dependent proteasome activity inhibition (Fig. 3). Free BTZ and BP quickly inhibited more than 75% proteasome activity at 1 h, gradually increasing to more than 90% at 18 h. HA-CCMs-BP though exhibiting relatively lower proteasome inhibition in LP-1 cells than free BTZ and BP at 1 and 4 h, induced effective inhibition of proteasome activity, comparable to free BTZ and BP, in 18 h. It is clear that HA-CCMs-BP is able to inhibit proteasome activity though a somewhat longer time is required, due to the fact that to take effects, BP has to be released from HA-CCMs-BP and further hydrolyzed to BTZ. Similar results have also been reported for liposomal BTZ prodrug to MM1S MM cells [21].

3.3. In vivo imaging and pharmacokinetics

The biodistribution of HA-CCMs-Cy5 was investigated by in vivo fluorescence imaging in mice bearing 200–300 mm^3 LP-1 tumors (Fig. S3). To see a clearer trend in tumor accumulation in time and effect of HA inhibition, we have cropped out LP-1 tumor sections. Fig. 4A shows notably high tumor accumulation of HA-CCMs-Cy5 at 4 h post *i.v.* injection. The strongest tumor Cy5 fluorescence was detected at 6 h post-injection. Tumor Cy5 fluorescence though remaining strong decreased gradually from 6 to 24 h, suggesting superior tumor-targetability of HA-CCMs to LP-1 tumors. In contrast, pretreating mice with free HA obviously weakened tumor Cy5 fluorescence, revealing that tumor accumulation of HA-CCMs is enhanced by HA-receptor mediated mechanism. The in vivo pharmacokinetic studies in mice indicated a long elimination half-life ($t_{1/2,\beta}$ = ca. 4.7 h) of HA-CCMs-Cy5 (Fig. 4B), which was much longer than that of free BTZ (0.21 h) [24].

3.4. In vivo therapeutic efficacy

Dose-limiting toxicity has seriously restricted the clinical application of BTZ [44,45]. We here studied the tolerability of HA-CCMs-BP in normal mice (Fig. S4). HA-CCMs-BP with escalated doses ranging from 15 to 25 mg BTZ equiv./kg was intravenously injected into mice. The mice body weights, survival and toxicity were

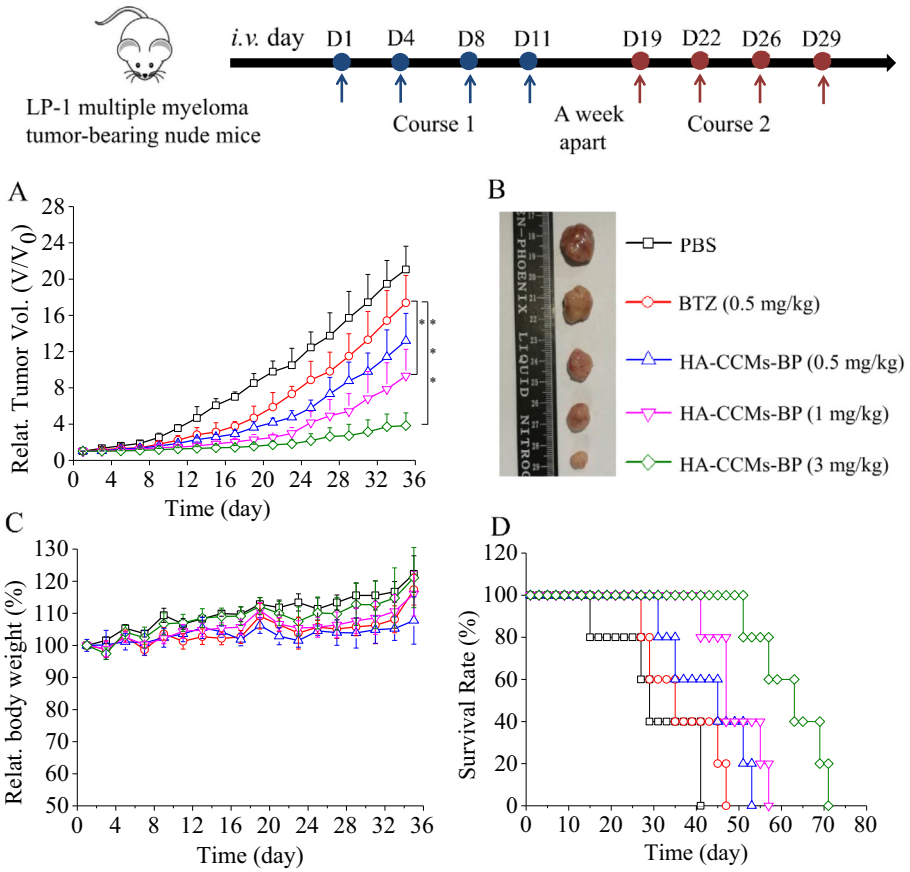

Fig. 5. *In vivo* antitumor performance of HA-CCMs-BP in LP-1 tumor-bearing nude mice. HA-CCMs-BP (dosage: 0.5, 1.0, or 3.0 mg BTZ equiv./kg) was given on day 1, 4, 8, 11, 19, 22, 26, and 29. PBS and free BTZ (dosage: 0.5 mg/kg) were used as controls. (A) Relative tumor volumes of mice from different treatment groups. Statistical analysis: One-way ANOVA with Tukey multiple comparison tests, $^{*}p < 0.05$, $^{***}p < 0.001$. (B) Photographs of typical tumor blocks collected on day 34. (C) Mice body weight changes in 34 d following different treatments. (D) Survival curves of mice in different treatment groups (n = 5). Kaplan-Meier analysis (log-rank test): HA-CCMs-BP (3 mg/kg) *vs.* BTZ and HA-CCMs-BP (0.5 mg/kg), $^{**}p < 0.01$; HA-CCMs-BP (3 mg/kg) *vs.* HA-CCMs-BP (1 mg/kg), $^{*}p < 0.05$.

monitored for 10 days. The results revealed that HA-CCMs-BP exhibited an extraordinarily high toleration of 20 mg/kg, which is approximately 20 times higher than free BTZ [24]. This high toleration of HA-CCMs-BP allows high-dose anti-tumor therapy with negligible side effects.

The therapeutic efficacy of HA-CCMs-BP was investigated in LP-1 tumor-bearing mice injected with HA-CCMs-BP (0.5, 1.0 or 3.0 mg/kg) or free BTZ (0.5 mg/kg). Drugs were given via the tail vein for 2 courses (first course on day 1, 4, 8, 11, and second course on day 19, 22, 26, 29) as clinical treatment. Fig. 5A reveals that free BTZ at a dose of 0.5 mg/kg induced little tumor growth inhibition. HA-CCMs-BP at the same dosage displayed apparently better tumor inhibition than free BTZ. Furthermore, meaningfully better tumor inhibition was obtained with growing dosages of HA-CCMs-BP to 1.0 and 3.0 mg BTZ. The tumor inhibition rate (TIR) was 17.5% for free BTZ while 36.1%, 55.7% and 81.8% for HA-CCMs-BP at 0.5, 1 and 3 mg BTZ equiv./kg, respectively. Fig. 5B confirmed that HA-CCMs-BP at a dose of 3 mg/kg achieved the best suppression of tumor growth. Fig. 5C shows that mice in all groups had scarce loss of body weight, demonstrating that all the treatments are well tolerated. In contrast, the treatment studies using free BTZ at a dosage of 1.0 mg/kg showed significant body weight loss (Fig. S5A), confirming that free BTZ possesses a pronounced systemic toxicity [24]. Liposomal BTZ prodrug though reported to cause effective inhibition of MM1S multiple myeloma xenografts at a dosage of 1.0 mg BTZ equiv./kg also induced about 10% mice body weight loss [21]. Free BTZ treatment at 0.5 mg/kg only induced slight improvement on survival time compared with PBS (median survival times: 34 *vs* 28 days) (Fig. 5D). All mice died in 8 days at an increasing dosage of 1.0 mg/kg (Fig. S5B). Notably, significantly longer median survival times of 44 and 62 days were recorded for HA-CCMs-BP at 0.5 and 3.0 mg BTZ equiv./kg, respectively. In comparison, only slight improvement of median survival time was observed for BTZ-loaded bone-targeting PEG-PLGA

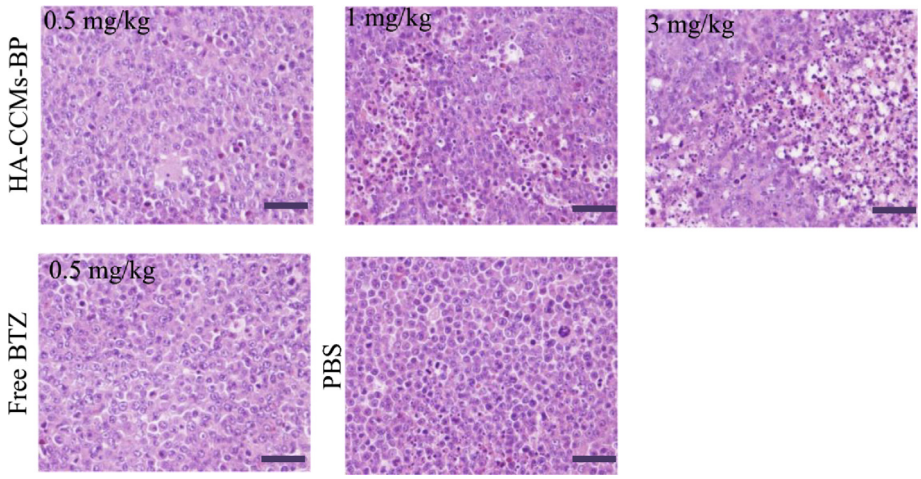

Fig. 6. H&E staining assays of tumors from different treatment groups on day 34. The images were obtained under Olympus BX41 microscope using a 40 × objective. Scale bar: 50 μm.

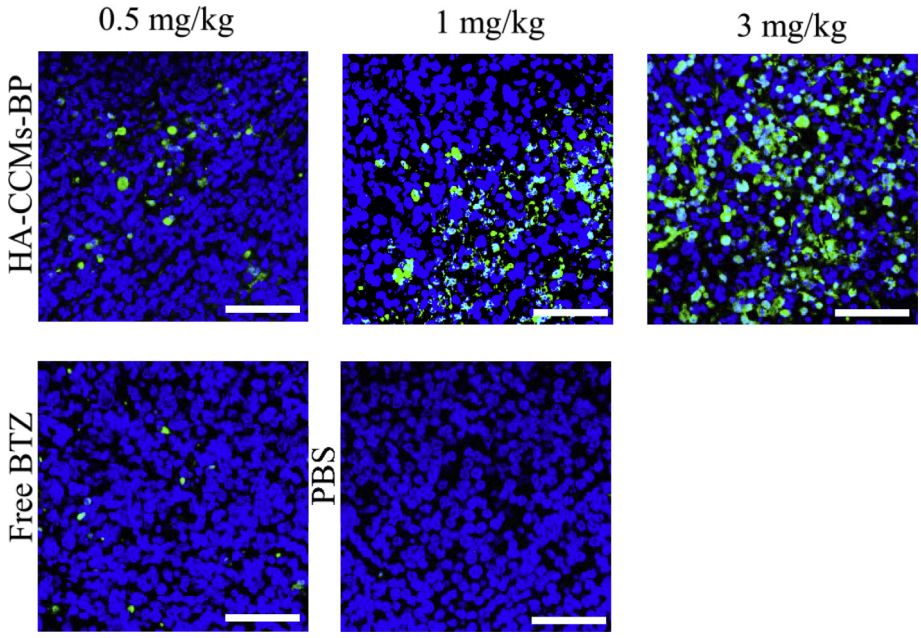

Fig. 7. Detection of apoptosis in the tumor tissue using the TUNEL assay. Green: apoptotic cells; blue: DAPI-stained cell nuclei. Scale bar: 50 μm. (For interpretation of the references to colour in this figure legend, the reader is referred to the web version of this article.)

nanoparticles in MM1S MM mice model [15]. BTZ-loaded CD38 antibody-functionalized chitosan nanoparticles showed also only moderate increase of median survival time compared with free BTZ in MM1S tumor-bearing mice [46]. Gu et al. reported a highly sophisticated system, *i.e.* alendronate-decorated, platelet membrane-coated, tissue plasminogen activator (tPA)-immobilized and bortezomib-loaded dextran nanoparticles, with sequential targeting effect to the bone microenvironment and myeloma cells, induced significantly better tumor inhibition and improved median survival time as compared to free BTZ in NCI-H929 MM-bearing mice [47]. The images of H&E staining exposed that HA-CCMs-BP at 3.0 mg BTZ equiv./kg caused extensive necrosis in the tumor site (Fig. 6), but little damage was observed in the other major organs (Fig. S6). TUNEL images further corroborated that HA-CCMs-BP induced more significant apoptosis of LP-1 cells at increasing dosages from 0.5 to 3 mg BTZ equiv./kg (Fig. 7). In contrast, free BTZ brought about much less cell apoptosis. These results confirm that HA-CCMs-BP has significantly improved tolerability, targetability and tumor inhibition in LP-1 multiple myeloma tumor xenografts, leading to increased survival rate. The easy synthesis, high stability, enhanced drug loading and active targeting ability of HA-CCMs-BP render it a fascinating platform for targeted chemotherapy of multiple myeloma cancer.

4. Conclusion

We have demonstrated that hyaluronic acid-shelled and core-disulfide-crosslinked biodegradable micelles (HA-CCMs) enable high loading and targeted delivery of lipophilized bortezomib to multiple myeloma in vivo, leading to enhanced treatment efficacy compared with free bortezomib. Interestingly, HA-CCMs made of a single block copolymer have integrated many unique properties such as small size, excellent stability, long circulation time, enhanced accumulation in CD44-overexpressing multiple myeloma xenografts in mice, fast and selective internalization by multiple myeloma cells, and triggered intracellular drug release. Lipophilized bortezomib has a significantly lower cytotoxicity than bortezomib while following loading into HA-CCMs shows improved anticancer activity, approaching that of free bortezomib, in CD44-positive multiple myeloma cells. As a result, lipophilized bortezomib-loaded HA-CCMs exhibit enhanced toleration, broadened therapeutic window, and more effective growth suppression of CD44-overexpressed multiple myeloma in nude mice than free bortezomib. The concept of using hyaluronic acid-shelled and core-disulfide-crosslinked biodegradable micelles to deliver lipophilized bortezomib has opened a new avenue for targeted bortezomib therapy of multiple myeloma.

Acknowledgements

This work is financially supported by research grants from the National Natural Science Foundation of China (NSFC 51373113, 51633005 and 51873144).

Appendix A. Supplementary data

Supplementary data to this article can be found online at https://doi.org/10.1016/j.actbio.2018.09.022.

References

[1] P.S. Rosenberg, A. Best, W.F. Anderson, O. Landgren, Multiple myeloma will become a common cancer in the era of modern therapy, Cancer Res. 76 (2016). 5231 5231.
[2] B. Barlogie, A. Mitchell, R.F. Van, J. Epstein, G.J. Morgan, J. Crowley, Curing myeloma at last: defining criteria and providing the evidence, Blood 124 (2014) 3043–3051.
[3] J.F. San-Miguel, M.-V. Mateos, Can multiple myeloma become a curable disease?, Haematologica 96 (2011) 1246–1248
[4] S. Gandolfi, J.P. Laubach, T. Hideshima, D. Chauhan, K.C. Anderson, P.G. Richardson, The proteasome and proteasome inhibitors in multiple myeloma, Cancer Metast. Rev. 36 (2017) 561–584.
[5] E.E. Manasanch, R.Z. Orlowski, Proteasome inhibitors in cancer therapy, Nat. Rev. Clin. Oncol. 14 (2017) 417–433.
[6] M. Groll, C.R. Berkers, H.L. Ploegh, H. Ovaa, Crystal structure of the boronic acid-based proteasome inhibitor bortezomib in complex with the yeast 20S proteasome, Structure 14 (2006) 451–456.
[7] P.C. Trippier, C. McGuigan, Boronic acids in medicinal chemistry: anticancer, antibacterial and antiviral applications, MedChemComm 1 (2010) 183–189.
[8] J. Schrader, F. Henneberg, R.A. Mata, K. Tittmann, T.R. Schneider, H. Stark, G. Bourenkov, A. Chari, The inhibition mechanism of human 20S proteasomes enables next-generation inhibitor design, Science 353 (2016) 594–598.
[9] S. Arastu-Kapur, J.L. Anderl, M. Kraus, F. Parlati, K.D. Shenk, S.J. Lee, T. Muchamuel, M.K. Bennett, C. Driessen, A.J. Ball, C.J. Kirk, Nonproteasomal targets of the proteasome inhibitors bortezomib and carfilzomib: a link to clinical adverse events, Clin. Cancer Res. 17 (2011) 2734–2743.
[10] R. Oerlemans, N.E. Franke, Y.G. Assaraf, J. Cloos, I. van Zantwijk, C.R. Berkers, G. L. Scheffer, K. Debipersad, K. Vojtekova, C. Lemos, J.W. van der Heijden, B. Ylstra, G.J. Peters, G.L. Kaspers, B.A. Dijkmans, R.J. Scheper, G. Jansen, Molecular basis of bortezomib resistance: proteasome subunit beta5 (PSMB5) gene mutation and overexpression of PSMB5 protein, Blood 112 (2008) 2489–2499.
[11] J.P. Vanderloo, M.L. Pomplun, L.C. Vermeulen, J.M. Kolesar, Stability of unused reconstituted bortezomib in original manufacturer vials, J. Oncol. Pharm. Pract. 17 (2011) 400–402.
[12] L. Wang, C. Shi, F.A. Wright, D. Guo, X. Wang, D. Wang, R.J.H. Wojcikiewicz, J. Luo, Multifunctional telodendrimer nanocarriers restore synergy of bortezomib and doxorubicin in ovarian cancer treatment, Cancer Res. 77 (2017) 3293–3305.
[13] M. Wang, Y. Wang, K. Hu, N. Shao, Y. Cheng, Tumor extracellular acidity activated "off-on" release of bortezomib from a biocompatible dendrimer, Biomater Sci. 3 (2015) 480–489.
[14] W. Xu, J. Ding, L. Li, C. Xiao, X. Zhuang, X. Chen, Acid-labile boronate-bridged dextran-bortezomib conjugate with up-regulated hypoxic tumor suppression, Chem. Commun. 51 (2015) 6812–6815.
[15] A. Swami, M.R. Reagan, P. Basto, Y. Mishima, N. Kamaly, S. Glavey, S. Zhang, M. Moschetta, D. Seevaratnam, Y. Zhang, J. Liu, M. Memarzadeh, J. Wu, S. Manier, J. Shi, N. Bertrand, Z.N. Lu, K. Nagano, R. Baron, A. Sacco, A.M. Roccaro, O.C. Farokhzad, I.M. Ghobrial, Engineered nanomedicine for myeloma and bone microenvironment targeting, Proc. Natl. Acad. Sci. 111 (2014) 10287–10292.
[16] S. Shen, J. Liu, R. Sun, Y.H. Zhu, J. Wang, Delivery of bortezomib with nanoparticles for basal-like triple-negative breast cancer therapy, J. Control. Release 208 (2015) 14–24.
[17] S.I. Thamake, S.L. Raut, Z. Gryczynski, A.P. Ranjan, J.K. Vishwanatha, Alendronate coated poly-lactic-co-glycolic acid (PLGA) nanoparticles for active targeting of metastatic breast cancer, Biomaterials 33 (2012) 7164–7173.
[18] M.F. Frasco, G.M. Almeida, F. Santos-Silva, C. Pereira Mdo, M.A. Coelho, Transferrin surface-modified PLGA nanoparticles-mediated delivery of a proteasome inhibitor to human pancreatic cancer cells, J. Biomed. Mater. Res. A 103 (2015) 1476–1484.
[19] J. Shen, G. Song, M. An, X. Li, N. Wu, K. Ruan, J. Hu, R. Hu, The use of hollow mesoporous silica nanospheres to encapsulate bortezomib and improve efficacy for non-small cell lung cancer therapy, Biomaterials 35 (2014) 316–326.
[20] G. Zuccari, A. Milelli, F. Pastorino, M. Loi, A. Petretto, A. Parise, C. Marchetti, A. Minarini, M. Cilli, L. Emionite, D. Di Paolo, C. Brignole, F. Piaggio, P. Perri, V. Tumiatti, V. Pistoia, G. Pagnan, M. Ponzoni, Tumor vascular targeted liposomal-bortezomib minimizes side effects and increases therapeutic activity in human neuroblastoma, J. Control. Release 211 (2015) 44–52.
[21] J.D. Ashley, J.F. Stefanick, V.A. Schroeder, M.A. Suckow, T. Kiziltepe, B. Bilgicer, Liposomal bortezomib nanoparticles via boronic ester prodrug formulation for improved therapeutic efficacy in vivo, J. Med. Chem. 57 (2014) 5282–5292.
[22] J. Su, F. Chen, V.L. Cryns, P.B. Messersmith, Catechol polymers for pH-responsive, targeted drug delivery to cancer cells, J. Am. Chem. Soc. 133 (2011) 11850–11853.
[23] S. Wu, R. Qi, H. Kuang, Y. Wei, X. Jing, F. Meng, Y. Huang, pH-responsive drug delivery by amphiphilic copolymer through boronate-catechol complexation, ChemPlusChem 78 (2013) 175–184.
[24] K. Wu, R. Cheng, J. Zhang, F. Meng, C. Deng, Z. Zhong, Micellar nanoformulation of lipophilized bortezomib: high drug loading, improved tolerability and targeted treatment of triple negative breast cancer, J. Mater. Chem. B 5 (2017) 5658–5667.
[25] S. Ganesh, A.K. Iyer, D.V. Morrissey, M.M. Amiji, Hyaluronic acid based self-assembling nanosystems for CD44 target mediated siRNA delivery to solid tumors, Biomaterials 34 (2013) 3489–3502.
[26] K. Cohen, R. Emmanuel, E. Kisin-Finfer, D. Shabat, D. Peer, Modulation of drug resistance in ovarian adenocarcinoma using chemotherapy entrapped in hyaluronan-grafted nanoparticle clusters, Acs Nano 8 (2014) 2183–2195.
[27] Y. Zhong, F. Meng, C. Deng, X. Mao, Z. Zhong, Targeted inhibition of human hematological cancers in vivo by doxorubicin encapsulated in smart lipoic acid-crosslinked hyaluronic acid nanoparticles, Drug Deliv. 24 (2017) 1482–1490.

[28] H. Yan, J. Song, X. Jia, Z. Zhang, Hyaluronic acid-modified didecyldimethylammonium bromide/ d-a-tocopheryl polyethylene glycol succinate mixed micelles for delivery of baohuoside I against non-small cell lung cancer: in vitro and in vivo evaluation, Drug Deliv. 24 (2017) 30–39.
[29] Y. Yan, X. Zuo, D. Wei, Concise review: emerging role of CD44 in cancer stem cells: a promising biomarker and therapeutic target, Stem Cells Transl. Med. 4 (2015) 1033–1043.
[30] L. Jin, K.J. Hope, Q. Zhai, F. Smadja-Joffe, J.E. Dick, Targeting of CD44 eradicates human acute myeloid leukemic stem cells, Nat. Med. 12 (2006) 1167–1174.
[31] R. Quere, S. Andradottir, A.C. Brun, R.A. Zubarev, G. Karlsson, K. Olsson, M. Magnusson, J. Cammenga, S. Karlsson, High levels of the adhesion molecule CD44 on leukemic cells generate acute myeloid leukemia relapse after withdrawal of the initial transforming event, Leukemia 25 (2011) 515–526.
[32] Y. Zhu, J. Zhang, F. Meng, L. Cheng, J. Feijen, Z. Zhong, Reduction-responsive core-crosslinked hyaluronic acid-b-poly(trimethylene carbonate-co-dithiolane trimethylene carbonate) micelles: synthesis and CD44-mediated potent delivery of docetaxel to triple negative breast tumor in vivo, J. Mater. Chem. B 6 (2018) 3040–3047.
[33] M. Li, Z. Tang, S. Lv, W. Song, H. Hong, X. Jing, Y. Zhang, X. Chen, Cisplatin crosslinked pH-sensitive nanoparticles for efficient delivery of doxorubicin, Biomaterials 35 (2014) 3851–3864.
[34] C.J. Rijcken, C.J. Snel, R.M. Schiffelers, C.F. van Nostrum, W.E. Hennink, Hydrolysable core-crosslinked thermosensitive polymeric micelles: synthesis, characterisation and in vivo studies, Biomaterials 28 (2007) 5581–5593.
[35] B. Sun, C. Deng, F. Meng, J. Zhang, Z. Zhong, Robust, active tumor-targeting and fast bioresponsive anticancer nanotherapeutics based on natural endogenous materials, Acta Biomater. 45 (2016) 223–233.
[36] Y. Zhong, J. Zhang, R. Cheng, C. Deng, F. Meng, F. Xie, Z. Zhong, Reversibly crosslinked hyaluronic acid nanoparticles for active targeting and intelligent delivery of doxorubicin to drug resistant CD44+ human breast tumor xenografts, J. Control. Release 205 (2015) 144–154.
[37] Y. Zhang, K.Q. Wu, H.L. Sun, J. Zhang, J.D. Yuan, Z.Y. Zhong, Hyaluronic acid-shelled disulfide-cross-linked nanopolymersomes for ultrahigh-efficiency reactive encapsulation and CD44-targeted delivery of mertansine toxin, ACS Appl. Mater. Interfaces 10 (2018) 1597–1604.
[38] Y. Fang, W. Yang, L. Cheng, F. Meng, J. Zhang, Z. Zhong, EGFR-targeted multifunctional polymersomal doxorubicin induces selective and potent suppression of orthotopic human liver cancer in vivo, Acta Biomater. 64 (2017) 323–333.
[39] A. Cadete, M.J. Alonso, Targeting cancer with hyaluronic acid-based nanocarriers: recent advances and translational perspectives, Nanomedicine 11 (2016) 2341–2357.
[40] F. Dosio, S. Arpicco, B. Stella, E. Fattal, Hyaluronic acid for anticancer drug and nucleic acid delivery, Adv. Drug Deliv. Rev. 97 (2016) 204–236.
[41] N.V. Rao, Y.Y. Hong, H.S. Han, H. Ko, S. Son, M. Lee, H. Lee, D.G. Jo, Y.M. Kang, J. H. Park, Recent developments in hyaluronic acid-based nanomedicine for targeted cancer treatment, Expert Opin. Drug Del. 13 (2016) 239–252.
[42] H. Wang, P. Agarwal, S. Zhao, R.X. Xu, J. Yu, X. Lu, X. He, Hyaluronic acid-decorated dual responsive nanoparticles of Pluronic F127, PLGA, and chitosan for targeted co-delivery of doxorubicin and irinotecan to eliminate cancer stem-like cells, Biomaterials 72 (2015) 74–89.
[43] N. Misaghian, G. Ligresti, L.S. Steelman, F.E. Bertrand, J. Basecke, M. Libra, F. Nicoletti, F. Stivala, M. Milella, A. Tafuri, M. Cervello, A.M. Martelli, J.A. McCubrey, Targeting the leukemic stem cell: the Holy Grail of leukemia therapy, Leukemia 23 (2009) 25–42.
[44] A. Russo, G. Bronte, F. Fulfaro, G. Cicero, V. Adamo, N. Gebbia, S. Rizzo, Bortezomib: a new pro-apoptotic agent in cancer treatment, Curr. Cancer Drug Tar. 10 (2010) 55–67.
[45] R.C. Kane, A.T. Farrell, R. Sridhara, R. Pazdur, United States Food and Drug Administration approval summary: bortezomib for the treatment of progressive multiple myeloma after one prior therapy, Clin. Cancer Res. 12 (2006) 2955–2960.
[46] P. de la Puente, M.J. Luderer, C. Federico, A. Jin, R.C. Gilson, C. Egbulefu, K. Alhallak, S. Shah, B. Muz, J. Sun, J. King, D. Kohnen, N.N. Salama, S. Achilefu, R. Vij, A.K. Azab, Enhancing proteasome-inhibitory activity and specificity of bortezomib by CD38 targeted nanoparticles in multiple myeloma, J. Control. Release 270 (2018) 158–176.
[47] Q. Hu, C. Qian, W. Sun, J. Wang, Z. Chen, H.N. Bomba, H. Xin, Q. Shen, Z. Gu, Engineered nanoplatelets for enhanced treatment of multiple myeloma and thrombus, Adv. Mater. 28 (2016) 9573–9580.